



FERROFLUID DROPLET VAPORIZATION IN A TRANSIENT ENVIRONMENT UNDER A LARGE MAGNETIC POWER.

Maycol Marcondes Vargas (myl_vargas@hotmail.com)

Cesar Flaubiano da Cruz Cristaldo (profcristaldo@yahoo.com.br)

Fernando Fachini Filho (fachini@lcp.inpe.br)

Grupo de Mecânica de Fluidos Reativos - Laboratório de Combustão e Propulsão - Instituto Nacional de Pesquisas Espaciais - 12630-000 - Cachoeira Paulista - SP

Abstract. *In this work the influence of transient processes of the gas phase on the vaporization of isolated ferrofluid droplet with spherical symmetry under the influence of an external alternating magnetic field is studied. Dispersed magnetic nanoparticles inside the droplet act as a heat source. The nanoparticle dipole reacts to the alternating magnetic field rotating the nanoparticle. The friction between the rotating nanoparticle and the surrounding liquid produces heat (viscous dissipation). Brownian motion of the liquid molecules is responsible for the nanoparticle dipoles misalignment when the magnetic field amplitude is null. Therefore, in each cycle of the magnetic field the nanoparticle rotates, generating heating in the core of the liquid. Applying this process on droplets is possible to reduce the droplet heating time. The conditions addressed in this problem leads to the magnetic power to be much larger than the thermal power, provided by the heat flux from the gas phase. The characteristic of this problem is a thermal boundary layer established close to the droplet surface in the liquid side. The results show an increase on vaporization rate with magnetic field frequency.*

Keywords: *Droplet vaporization, magnetic heating, ferrofluid*

1. Introduction

Spray combustion is the most used energy source nowadays. That is the main motivation to understand mechanisms controlling the spray combustion. One of the most important mechanisms to start understanding is the isolated droplet combustion. Heating and vaporization of isolated droplets are controlled mainly by the heat flux from the gas phase. Another important mechanism is the atomization, because from it liquid fuels are broken into a very large number of very small droplets, which have a very large contact area between the gas and liquid phases. Then the heat flux from the gas phase to the liquid phase becomes high enough to provide high droplet heating and vaporization rates which make the liquid fuel burning efficient. Recently, the magnetic relaxation heating is included in the ferrofluid droplet problem in order to increase the heating and vaporization rates, (Cristaldo and Fachini, 2013a,b). In this work the effect of the transient processes of the gas phase on the ferrofluid droplet problem is studied.

Low fuel consumption and low pollutant emission for liquid fuel combustion demand a continuous search for new processes in order to reduce droplet heating time, to increase the droplet vaporization rate and to improve reactants mixing. One way of enhancing the combustion process is made by enhancing the fluid transport properties. For that, metal particles are disposed in the liquid fuel, and such composition is denominated slurry. Slurries have higher thermal conductivities than pure fuels, however this kind of fluids are very abrasive, which restrict their use, (Das *et al.*, 2003).

An alternative for slurries are nanofluids. This new class of fluid consists of liquid (carriers) containing stable dispersed surface-coated nanoparticles with diameter smaller than 100 nm. As example, by introducing small quantities of copper nanoparticles, carbon nanotubes, magnetite nanoparticles or others colloidal nanoparticles into the fluid, thermal enhancement has been found (Eastman *et al.*, 2001; Choi *et al.*, 2001; Koblinski *et al.*, 2008; Shima *et al.*, 2009; Tyagi *et al.*, 2008; Yetter *et al.*, 2009; Philip *et al.*, 2007). Applications for these kind of fluids can be found in automotive industry as coolant, fuel additives and lubricant. Also improvements in heat transfer is found due to the replacement of water with nanofluids in automobile radiator, (Peyghambarzadeh *et al.*, 2011).

Among nanofluids, ferrofluids are a special case. Ferrofluids present magnetic properties due to the magnetic characteristic of their nanoparticles. That characteristic permits the ferrofluid to respond to an external magnetic field. The most important response to the combustion field is the magneto relaxation heating, (Fachini and Bakuzis, 2010; Cristaldo and Fachini, 2013a,b). This process is generated by the response of the magnetic nanoparticle to the external magnetic field. Each magnetic nanoparticle tends to align its dipole with the magnetic field, which induces the rotation of the nanoparticle. This movement occurs against the molecular forces, and the result is heat generation due friction (viscous dissipation). In the case of an external alternating magnetic field, the nanoparticles align with the magnetic field and they are misaligned by the collision with the fluid molecules (Brownian motion). Thus in each cycle of the magnetic field the nanoparticle generates heat in the core of the liquid.

Recently the magneto relaxation heating is applied on droplet combustion problems, (Fachini and Bakuzis, 2010; Cristaldo and Fachini, 2013a,b). The condition addressed in the previous analysis leads to the magnetic power much larger than the thermal power provided by the heat flux from the gas phase to the liquid phase. Under these conditions, the heating time is drastically reduced, but is still much larger than the characteristic time of the process in the gas phase.

Therefore the quasi-steady models for the gas phase are still valid (Cristaldo and Fachini, 2013a,b).

Since the droplet heating time becomes comparable to the characteristic time of the gas phase for the condition of very high magnetic power, the transient process of the gas phase may be an important effect on heating and vaporization of isolated droplets. In this analysis, the droplet problem is analyzed considering the transient effects of the gas phase.

2. Mathematical Formulation

The problem configuration consists of a single ferrofluid fuel droplet being heated by the heat flux provided by the gas phase and an alternating magnetic field. The droplet is in a quiescent atmosphere and has spherical symmetry, permitting the problem to be treated as one dimensional. The droplet vaporization problem is divided in two domains (liquid - gas), and a set of conservation equations are used to describe each one. The liquid phase has the droplet radius a_0^* (radius) and temperature T_0 as the initial conditions. Liquid density ρ_l^* , boiling temperature T_b^* , specific heat c_l^* and thermal conductivity k_l^* are constants. The gas phase is composed by a mixture of air and fuel vapor $Y_{F\infty}^*$, with temperature T_∞ , density ρ_∞^* , specific heat capacity c_p^* and thermal conductivity $k_{g\infty}^*$ also constants. Lewis number in the gas phase is equal to unity and heat transfer due radiation is neglected. The problem equations are non-dimensionalized by the following variables.

Independent variables:

$$r \equiv r^*/a_0^*, \quad t \equiv t^*/t_h^*$$

Dependent variables:

$$a \equiv a^*/a_0^*, \quad T \equiv T^*/T_b^*, \quad u \equiv u^*/(\alpha_\infty^*/a_0^*), \quad \rho \equiv \rho^*/\rho_\infty^*, \quad Y_F \equiv Y_F^*/Y_{F\infty}^*$$

where r , t , a , T , u , ρ and Y_F stand for: radial coordinate, time, droplet radius, temperature, gas velocity, density and fuel mass fraction respectively. Time t^* is non-dimensionalized by a characteristic time, in this case, the heating time estimative $t_h^* \equiv \rho_l^* a_0^{*2} / (\rho_\infty^* \alpha_\infty^*)$, in which $\alpha_\infty^* \equiv k_{g\infty}^* / c_p^* \rho_\infty^*$ is the thermal diffusivity. The dimensional variables are denoted by the superscript * whereas the subscripts b and ∞ represent the boiling and ambient conditions, respectively.

2.1 Liquid Phase

For describing the liquid phase, non-dimensional equations of mass conservation and energy balance are used, (Fachini and Bakuzis, 2010; Cristaldo and Fachini, 2013a):

$$\frac{da^3}{dt} = -3\lambda \quad (1)$$

and

$$\frac{\partial T}{\partial t} - \frac{A}{r^2} \frac{\partial}{\partial r} \left(r^2 \frac{\partial T}{\partial r} \right) = P_m \frac{f^2 \tau_r(T)}{1 + [f \tau_r(T)]^2} \quad (2)$$

having the following boundary conditions:

$$\frac{\partial T}{\partial r} = 0 \quad (3)$$

$$r^2 T^n \frac{\partial T}{\partial r} \Big|_{a^+} = \lambda L + r^2 A \frac{\partial T}{\partial r} \Big|_{a^-} \quad (4)$$

Equation (1) represents the mass conservation equation in its non-dimensional form, where $\lambda(t) \equiv \dot{m}^*(t^*) c_p^* / (4\pi k_{g\infty}^*)$ is the non-dimensional vaporization rate, in which $\dot{m}^*(t^*)$ is the dimensional vaporization rate, $A \equiv c_p^* k_l^* / c_l^* k_{g\infty}^*$ is a constant and τ_r is the dimensionless magneto relaxation time. Equation (2) represents the energy balance equation. The right hand side of equation (2) represents the energy dissipation due to the rotation of the magnetic nanoparticles (magnetic heating). Equation (3) is a symmetry condition imposed in the droplet core, and equation (4) is the heat conservation at the droplet surface. The gas thermal conductivity is a function of the temperature $k_g/k_{g\infty} = T^n$, with $n = 0.5$. The non-dimensional latent heat of vaporization is defined as $L \equiv L^* / (c_p^* T_b^*)$ and it is assumed constant in this work. The subscript a^- represents a region at the droplet surface in the liquid side, while a^+ represents a region at the surface in the gas side.

The magnetic heating rate is given by the characteristic time of misalignment of the dipoles (effective relaxation time), defined as $t_m^{*-1} = t_B^{*-1} + t_N^{*-1}$, in which t_B^{*-1} is the Brownian relaxation time and t_N^{*-1} is the Néel relaxation time. Brownian mechanism considers the rotation of the entire particle, where the rotation generates heat due the friction between the fluid and the magnetic nanoparticle. Néel mechanism consists of considering the rotation of the dipole inside of the nanoparticle (not the nanoparticle). In this work, the condition $t_B^{*-1} \ll t_N^{*-1}$ is assumed. More information are available in (Fachini and Bakuzis, 2010).

The P_m parameter is the ratio of magnetic heat source to the thermal energy source (provided by the gas phase), and can be described as:

$$P_m \equiv \frac{\mu_0 \chi_0 H_0^2 t_h^*}{2\rho_l^* c_l^* T_b^* t_{Bb}^*} \quad (5)$$

where μ_0 is the magnetic permeability, H_0 is the magnetic field amplitude and χ_0 is the initial susceptibility. More detailed information about these values and equations are shown in (Fachini and Bakuzis, 2010; Cristaldo and Fachini, 2013b).

Under such configuration, the magnetic energy dissipation inside the droplet is controlled by two main parameters, the magnetic parameter P_m and the field frequency $f \equiv 2\pi f^* t_{Bb}^*$, in which f^* is the dimensional frequency, and t_{Bb}^* is the effective relaxation time determined at the boiling temperature.

The assumption of a very high magnetic parameter is used in this work, $P_m \gg 1$, implying in first approximation a uniform temperature profile inside the droplet, according to Eq. (2). In order to describe properly the temperature profile, a thermal boundary layer must be considered. This thermal boundary layer is responsible for matching the uniform temperature profile in the core with the gas phase temperature profile. For the matching it is necessary to re-scale the temporal and spatial coordinates to follow the evolution of temperature inside the thermal boundary layer. The appropriate time scale is $t \sim 1/P_m$, then the new time is $\tau \equiv tP_m$. Re-scaling the spatial coordinate leads to $r = a + \delta x$, where $x = O(1)$ and $\delta \ll 1$. After the transformation the system of Eqs. (1) to (4) becomes:

$$\frac{da^3}{d\tau} = -3 \frac{\lambda}{P_m} \quad (6)$$

$$\frac{\partial T}{\partial \tau} = \frac{\partial^2 T}{\partial x^2} + \frac{f^2 T}{T^2 + f^2} \quad (7)$$

with the boundary conditions:

$$\frac{\partial T}{\partial x} = 0 \quad \text{at} \quad x \rightarrow -\infty \quad (8)$$

and

$$a^2 T^n \left. \frac{\partial T}{\partial r} \right|_{a^+} = \lambda L + a^2 (AP_m)^{1/2} \left. \frac{\partial T}{\partial x} \right|_{0^-} \quad \text{at} \quad r = a \quad (9)$$

2.2 Gas Phase

The non-dimensional conservation equations to describe the gas phase are:

$$p_m \frac{\partial \rho}{\partial \tau} + \frac{1}{r^2} \frac{\partial}{\partial r} (r^2 \rho u) = 0 \quad (10)$$

$$p_m \frac{\partial (\rho T)}{\partial \tau} + \frac{1}{r^2} \frac{\partial}{\partial r} (r^2 \rho u T) - \frac{1}{r^2} \frac{\partial}{\partial r} \left(r^2 T^n \frac{\partial T}{\partial r} \right) = 0 \quad (11)$$

$$p_m \frac{\partial (\rho Y_F)}{\partial \tau} + \frac{1}{r^2} \frac{\partial}{\partial r} (r^2 \rho u Y_F) - \frac{1}{r^2} \frac{\partial}{\partial r} \left(\frac{r^2 T^n}{Le_F} \frac{\partial Y_F}{\partial r} \right) = 0 \quad (12)$$

in which $p_m \equiv \varepsilon P_m$ and $\varepsilon \equiv \rho_\infty^* / \rho_l^*$ is the ratio of gas phase density to liquid phase density. Density ratio is chosen equal to: 10^{-4} , 10^{-3} , 10^{-2} , 2×10^{-2} and 5×10^{-2} . This variation is used to simulate different gas phase conditions. Le_F is the vapor Lewis number and Y_F is the fuel mass fraction.

The boundary conditions of the gas phase is:

$$\frac{r^2 T^n}{Le_F} \left. \frac{\partial Y_F}{\partial r} \right|_{a^+} = \lambda (Y_{F_s} - 1) \quad \text{at} \quad r = a \quad (13)$$

Y_{F_s} is the mass fraction at the liquid-gas interface, where the subindex s stands for the condition at the droplet surface, and it is calculated by use of the Clausius-Claperyon relation:

$$Y_{F_s} = exp \left[\gamma \left(1 - \frac{1}{T_s} \right) \right] \quad (14)$$

where $\gamma \equiv L^* M_F^* / (R_0^* T_b^*)$ is a function of the latent heat of vaporization L^* , the fuel molecular weight M_F^* , the universal gas constant R_0^* and the boiling temperature T_b^* .

Far from the droplet the following conditions are assumed:

$$T = T_\infty \quad \text{and} \quad Y_F = 0 \quad \text{at} \quad r \rightarrow +\infty \quad (15)$$

2.3 Numerical Strategy

The problem is solved considering a n-heptane ferrofluid droplet in a quiescent inert atmosphere with temperature T_∞ and vapor mass fraction Y_F . Three different temperatures are considered for the ambient temperature T_∞ . The problem is numerically solved by following the procedure:

1. An initial guess for the vaporization rate λ and the surface temperature T_s are provided.
2. Temperature and mass fraction profiles are determined by integrating Eqs (7),(11) and (12) with the gas properties. The differential equations are solved by an explicit finite difference scheme.
3. Once the temperature and mass fraction are known, the boundary conditions Eqs. (9) and (13) are calculated. If they are not satisfied, new vaporization rate λ and new surface temperature T_s are chosen via Newton-Raphson method. The process is repeated until the boundary conditions Eqs. (9) and (13) to be satisfied.
4. At this point, the process advances to the next time step. Since $P_m \ll 1$, the radius variation is very small for $\tau = O(1)$. The effect the variation of magnetic nanoparticle fraction can be neglected during the heating process.
5. The process is repeated until any point inside the droplet to reach boiling temperature.

3. Results and Discussion

The fuel used in this problem is n-heptane with boiling temperature (T_b^*) equal to 371.55 K. The initial temperature (T_0^*) is the same for all cases, being equal to 297.24 K ($T = 0.8$). Properties of nanoparticles like domain magnetization, magnetic permeability and volume fraction of magnetic nanoparticles are all included into the parameter P_m . The model simulates the droplet vaporization until any point inside the droplet reaches the boiling condition ($T = 1$). The model does not hold for temperature higher than one ($T > 1$) because of the bubble formation inside the droplet.

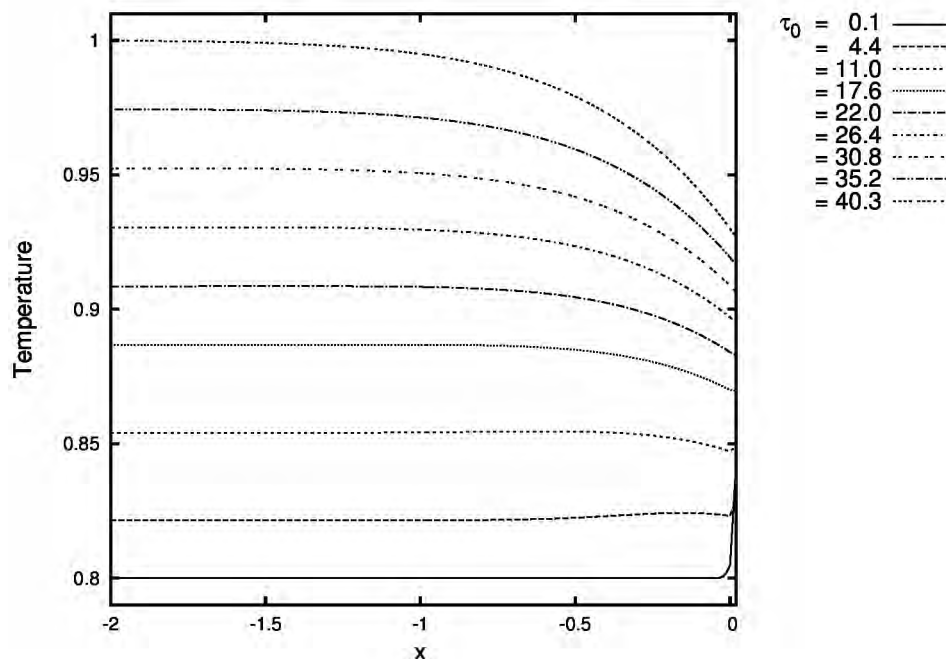


Figure 1. Temporal evolution of temperature profiles inside the droplet. $T_\infty = 0.9$, $f = 1.0$ and $p_m = 1.0$

Vapor mass fraction far from the droplet is constant for all cases ($Y_F^* = 0$, then $Y_F = Y_F^*$). All the processes are simulated for Lewis number equal unit.

The frequency is varied from $f = 0.3$ to values in which relaxation processes of the nanoparticles reaches saturation ($f \sim 5$). For frequencies lower than 0.3, the thermal boundary layer model becomes not valid, i.e., thickness becomes of the same order of the droplet radius, $\delta = (A/P_m f^2)^{1/2} = 0$.

As observed previously (Cristaldo and Fachini, 2013a), the magnetic source increases with the frequency, consequently droplet heating time is reduced as the magnetic field frequency increases. The results of previous work (Cristaldo and Fachini, 2013a) are based on $p_m = 0$, but in the current analysis p_m will take values different from zero, specifically $p_m = 0.01, 0.1, 1, 2$ and 5. Therefore, the effect of transient processes in the gas phase on the droplet heating evolution

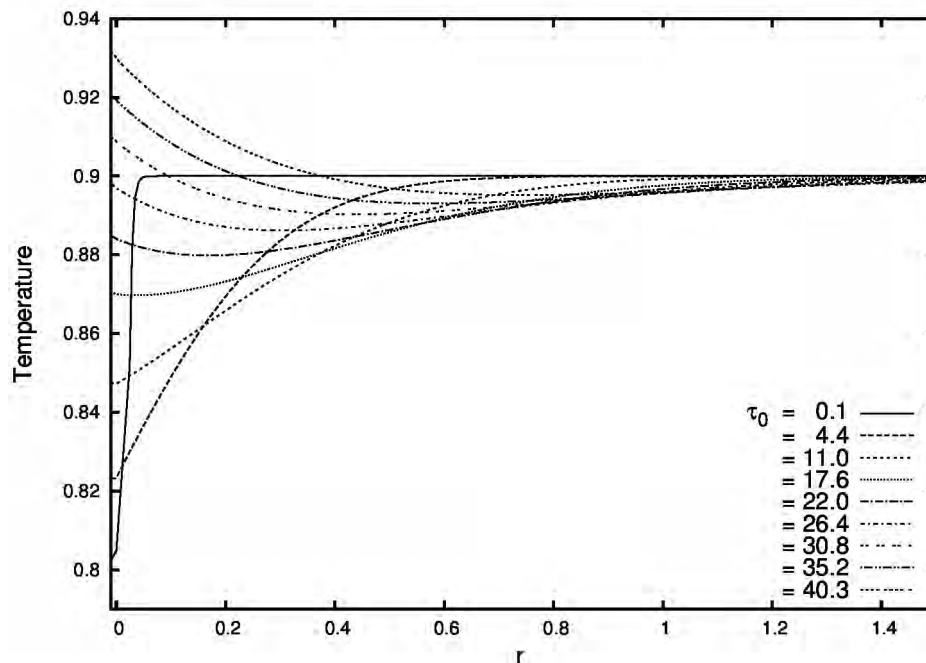


Figure 2. Temporal evolution of temperature profiles inside the droplet. $T_\infty = 0.9$, $f = 1.0$ and $p_m = 1.0$

and vaporization rate may be evaluated. For the p_m parameter present in Eqs (10),(11) and (12), is assumed the values of 0.01, 0.1, 1.0, 2.0 and 5.0.

It is important to highlight the magnetic relaxation heating. Since P_m is a fixed value, $P_m = 100$, each p_m corresponds to different values of the ratio of liquid-gas density ε . In addition for each p_m there is a different time scale. Therefore to compare results from cases with different p_m a common heating time scale must be considered. For that, the heating time for $\varepsilon = \varepsilon_0 = 10^{-4}$ is used. The correlation between the each time scale to that one corresponding to ε_0 is $\tau = \tau_0 \varepsilon$.

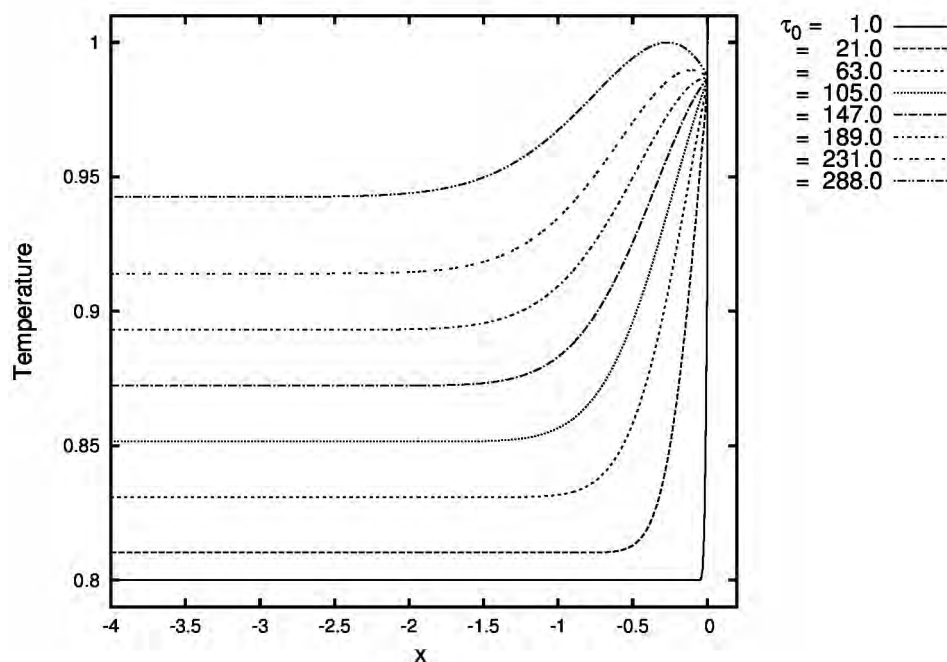


Figure 3. Temporal evolution of temperature profiles inside the droplet. $T_\infty = 6.0$, $f = 1.0$ and $p_m = 1.0$

Figure 1 shows the time evolution of the temperature profile inside the droplet for low ambient temperature ($T_\infty = 0.9$). In this figure it is seen that the boiling temperature is reached at the the droplet core. Also, this case shows that a heat flux from the droplet core to the droplet surface, indicating the magneto relaxation heating as a heat source for heating the

droplet. Figure 2 shows the gas phase of the same case described in Fig. 1. It is seen that the presence of droplet with low temperature in an ambient with temperature lower than the boiling temperature cools the gas phase surrounding it during the whole heating time.

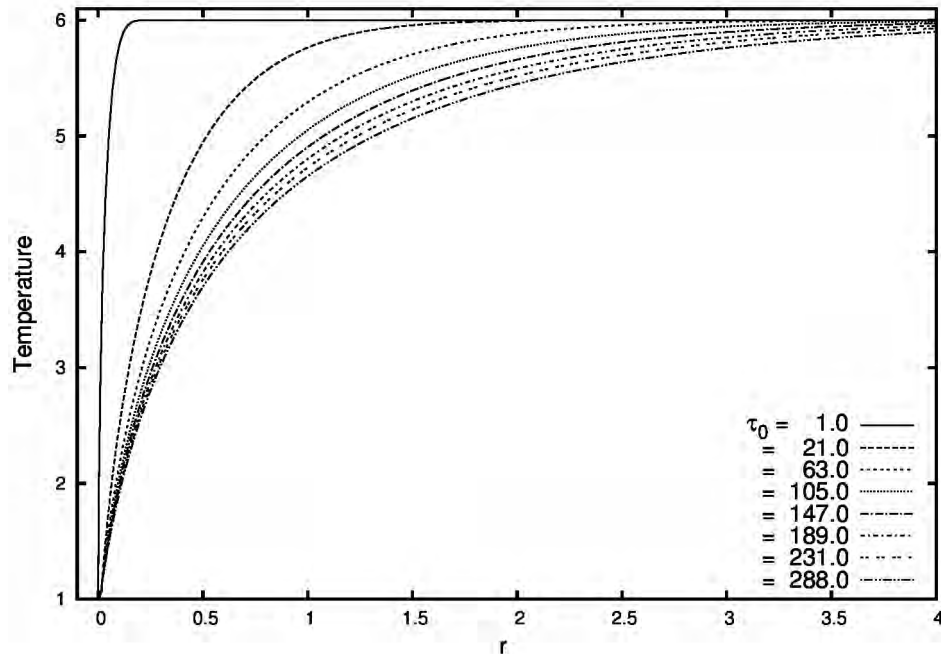


Figure 4. Temporal evolution of temperature profiles in the gas phase. $T_\infty = 6.0$, $f = 1.0$ and $p_m = 1.0$

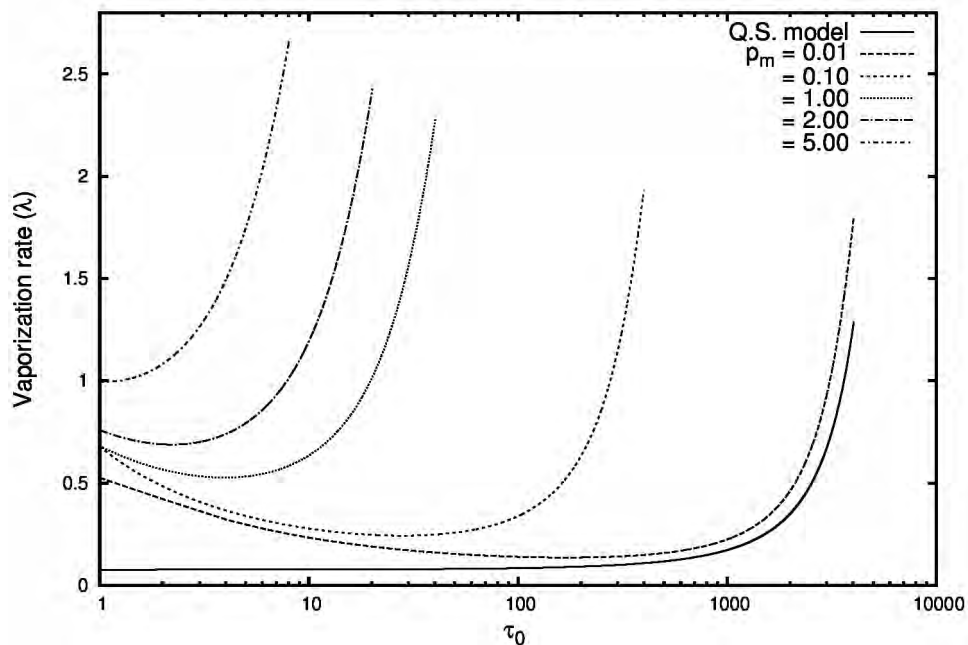


Figure 5. Time evolution of the vaporization rate for different p_m . $T_\infty = 0.9$

Figure 3 shows the evolution of temperature profile inside the droplet thermal boundary layer for a high ambient temperature. In this figure it is demonstrated that the boiling temperature condition ($T = 1$) is reached inside the droplet close to the droplet surface. Notice that droplet surface temperature changes very little for $\tau_0 > 1$ indicating an surface temperature evolution in very short time period for the case of $T_\infty = 0$. Figure 4 shows the cooling of the gas phase caused by the droplet presence in a high temperature environment.

Figure 5 exhibits temporal evolution of the vaporization rate for different values for p_m . It is noted an augment in the vaporization rate with p_m . Examining Eqs (11) and (12), it is noticed an increase in the value of p_m results in the transient term, meaning a small mass and heat accumulation in the gas phase. This fact leads to high heat and mass flux from/to

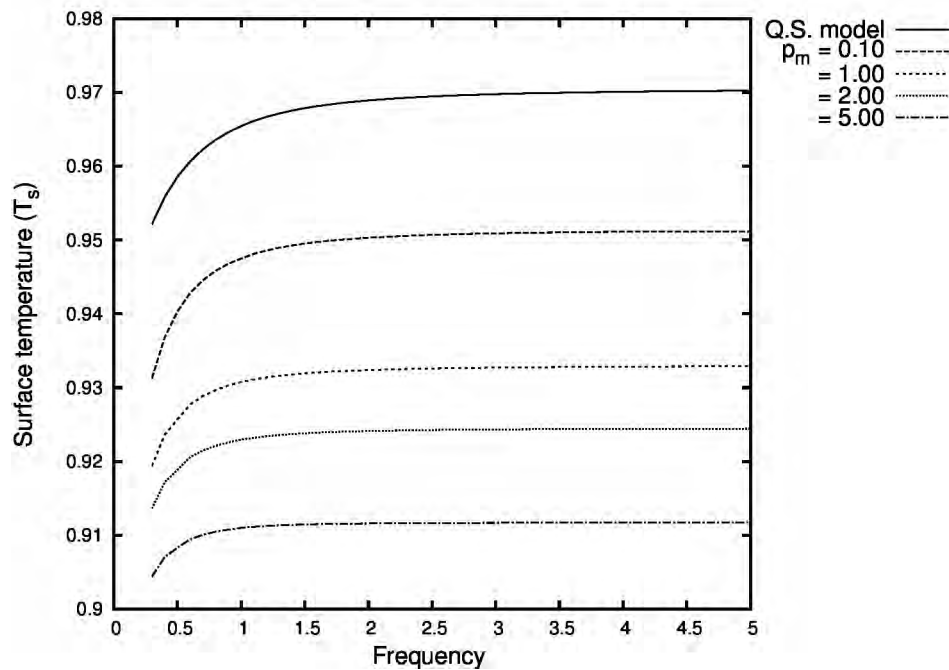


Figure 6. Surface temperature for different p_m in function of the magnetic field frequency. $T_\infty = 0.9$

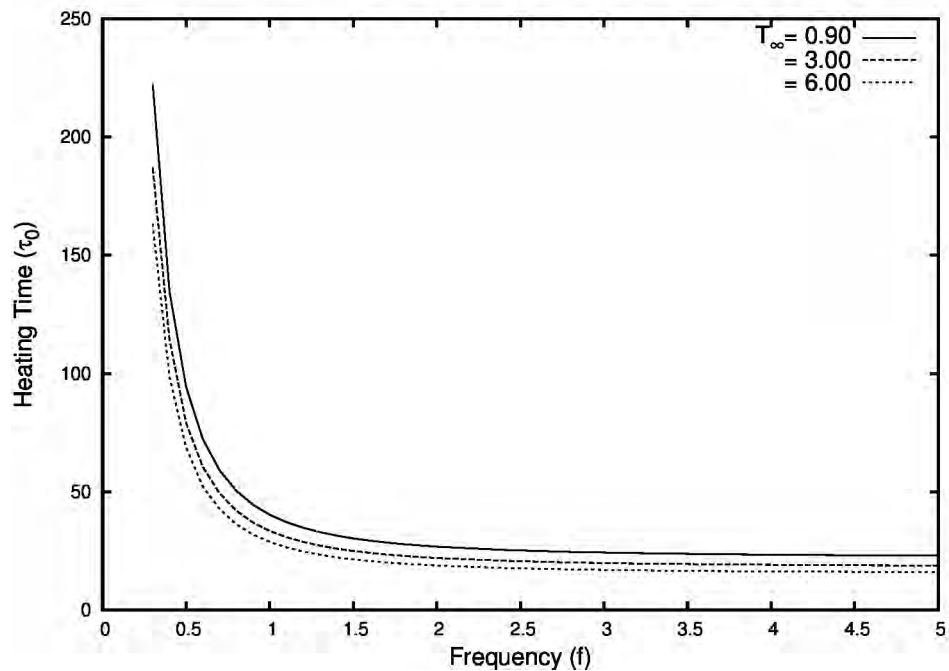


Figure 7. Heating time in function of the frequency for different temperatures.

the gas phase at the droplet surface. Consequently, increasing the value of p_m , there is an increase in the vaporization rate which decreases the droplet surface temperature, as seen in Fig 6. Also, Figure 5 present two cases: $p_m = 0$ and $p_m = 0.01$. The case $p_m = 0$ corresponds to the quasi-steady for the processes in the gas phase, which is calculated in previous analysis (Cristaldo and Fachini, 2013b). Comparing the transient case $p_m = 0.01$ and the quasi-steady case $p_m = 0$, it is possible to say that the transient code is validated. In addition, Figure 5 exhibits a strong reduction on the heating time with p_m . The augment of the vaporization rate by increasing p_m occurs due to the augment of transient term influence in the heating and vaporization processes.

Figure 7 shows the droplet heating time as a function of the magnetic field frequency f for different gas phase temperatures ($T_\infty = 0.9, 3, 6$) for p_m equal to one. The heating time is much more sensitive to frequency variations than temperature variation. For the conditions of low frequencies ($f < 1.4$), the field frequency exerts great influence on determining the droplet heating time. For frequencies $f > 2$, the saturation regime for the magneto relaxation heating is reached.

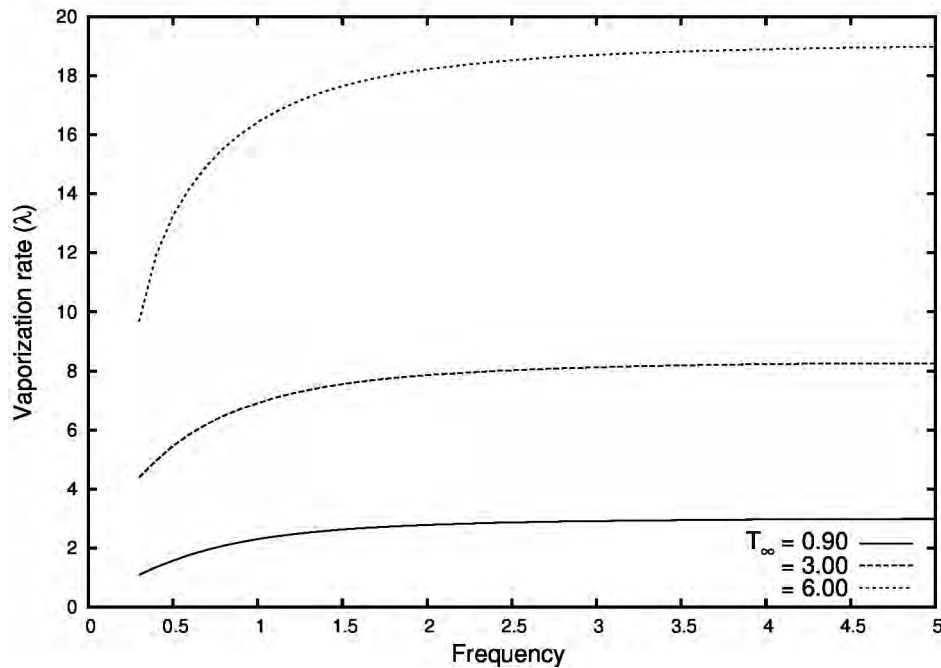


Figure 8. Vaporization rate in function of the frequency for different temperatures and $p_m = 1$.

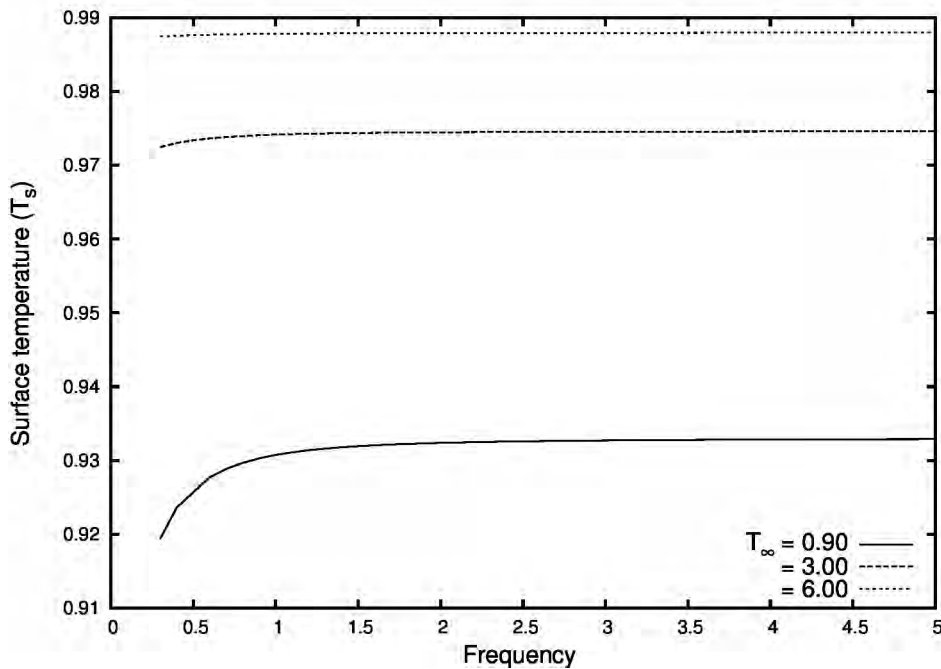


Figure 9. Surface temperature in function of the frequency for different temperatures and $p_m = 1$.

Figures 8 and 9, depict the influence of the ambient temperature T_∞ and the frequency f on the vaporization rate λ and the droplet surface temperature T_s . Reducing the heat flux from the gas phase to the droplet with a decrease of T_∞ , the effect of magneto relaxation heating dominates the process. This characteristic is confirmed analyzing the relative effect on the results of Fig. 8. For the case $T_\infty = 0.9$, augmenting the frequency the vaporization rate changes about three times, $\lambda(f = 0.3) \sim 1$ and $\lambda(f = 5) \sim 3$. Meanwhile, for the case $T_\infty = 6$, there is an increase about twice. In general, the vaporization rate is controlled by the ambient atmospheric temperature, as seen in Fig 8. Unlike vaporization rate, the droplet surface temperature T_s is mainly controlled by the ambient atmospheric temperature T_∞ , as seen in Fig 9.

All results exhibited in Figs. 8 and 9 correspond to values found in the instant when boiling condition is reached at any position inside the droplet.

22nd International Congress of Mechanical Engineering (COBEM 2013)
November 3-7, 2013, Ribeirão Preto, SP, Brazil

4. CONCLUSIONS

The results point out the strong influence of the magneto relaxation heating and vaporization processes in the droplet problem. The transient processes in the gas phase are significant on reducing the energy and mass accumulation in the gas phase around the droplet, which improve the fluxes of heat and mass, and consequently, the vaporization rate.

As seen in previous work, the boiling condition is found inside the droplet which can favor the formation of bubble and the disruption of the droplet. This situation can be an extra atomization process.

5. REFERENCES

- Choi, S.U.S., Zhang, Z.G., Yu, W., Lockwood, F.E. and Grulke, E.A., 2001. "Anomalous thermal conductivity enhancement in nanotube suspensions". *Appl. Phys. Lett.*, Vol. 79.
- Cristaldo, C.F.C. and Fachini, F.F., 2013a. "Asymptotic analysis of ferrofluid droplet combustion under very large magnetic power". *34th International Symposium on Combustion*, p. 18.
- Cristaldo, C.F.C. and Fachini, F.F., 2013b. "Ferrofluid droplet heating and vaporization under very large magnetic power: A thermal boundary layer model". *Physics of Fluids*, Vol. 25, No. 3.
- Das, S.K., Putra, N., Thiesen, P. and Roetzel, W., 2003. "Temperature dependence of thermal conductivity enhancement for nanofluids". *J. Heat Trans.*, Vol. 125, pp. 567 – 574.
- Eastman, J.A., Choi, S.U.S., Li, S., Yu, W. and Thompson, L., 2001. "Anomalous increased effective thermal conductivities of ethylene glycol-based nanofluids containing copper nanoparticles". *Appl. Phys. Lett.*, Vol. 78.
- Fachini, F.F. and Bakuzis, F., 2010. "Decreasing nanofluid droplet heating time with alternating magnetic fields". *J. Appl. Phys.*, Vol. 108, No. 084309.
- Kebllinski, P., Prasher, R. and Eapen, J., 2008. "Thermal conductance of nanofluids: is the controversy over?" *J. Nanopart. Res.*, Vol. 10.
- Peyghambarzadeh, S., Hashemabadi, S., Jamnani, M.S. and Hoseini, S., 2011. "Improving the cooling performance of automobile radiator with Al_2O_3 /water nanofluid". *Applied Thermal Engineering*, Vol. 31, No. 10, pp. 1833 – 1838.
- Philip, J., Shima, P.D. and Raj, B., 2007. "Enhancement of thermal conductivity in magnetite based nanofluid due to chainlike structures". *Appl. Phys. Lett.*, , No. 91.
- Shima, P.D., Philip, J. and Raj, B., 2009. "Role of microconvection induced by brownian motion of nanoparticles in the enhanced thermal conductivity of stable nanofluids". *Appl. Phys. Lett.*, Vol. 94.
- Tyagi, H., Phelan, P.E., Prasher, R., Peck, R., Pacheco, T.L.J.R. and Arentzen, P., 2008. "Increased hot-plate ignition probability for nanoparticle-laden diesel fuel". *Nano Lett.*, Vol. 8.
- Yetter, R.A., Rish, G.A. and Son, S.F., 2009. "Increased hot-plate ignition probability for nanoparticle-laden diesel fuel". *Proc. Combust. Inst.*, , No. 32.

6. RESPONSIBILITY NOTICE

The authors are the only responsible for the printed material included in this paper.